http://doi.org/10.29227/IM-2021-02-54 Received: 16 Jun 2021, Accepted: 18 Aug 2021, Published: 10 Nov 2021

Exploring the Relation between Seismic Coefficient and Rock Properties Through Field Measurements and Empirical Model for Evaluating the Effect of Blast-Induced Ground Vibration in Open-Pit Mines: A Case Study at the Thuong Tan III Quarry (Vietnam)

TRAN Quang Hieu[1, *]

[1] Hanoi University of Mining and Geology, 18 Viet street, Hanoi, Vietnam

Corresponding author: tranquanghieu@humg.edu.vn

Abstract Blasting is one of the most effective methods for fragmenting rock in quarries. Nevertheless, its adverse effects are significant, especially blast-induced ground vibration. Field measurement and empirical equations are simple methods to determine and estimate the intensity of blast-induced ground vibration. However, we cannot evaluate the effects of blast-induced ground vibration on the surrounding environment based on these outcomes. Therefore, this study explores the relation between seismic coefficient and rock properties through field measurements and an empirical model for evaluating the effect of blast-induced ground vibration in open-pit mines. Accordingly, the seismic coefficient (K) is considered the main objective in this study. Firstly, it was determined based on the rock properties. Subsequently, an empirical model for estimating blast-induced ground vibration was developed based on field measurements. This empirical equation was then expanded to determine K to check whether it matches the determined K by the rock properties. Finally, it was used as the threshold to determine the maximum explosive charged per delay to ensure the safety of the surrounding environment from blast-induced ground vibration. For this aim, the Thuong Tan III quarry (in Binh Duong province, Vietnam) was selected as a case study. Fifth-teen blasting events with a total of 75 blast-induced ground vibration values were recorded and collected. An empirical equation for estimating blast-induced ground vibration was then developed based on the collected dataset, and K was determined in the range of 539 to 713 for the Thuong Tan III quarry. Based on the measured blast-induced ground vibrations, developed empirical model, and K values, the Phase 2 software was applied to simulate the effects of blast-induced ground vibration on the stability of slopes as one of the impacts on the surrounding environment. From the simulation results, we can determine the maximum explosive charged per delay for each type of rock to ensure the stability of the slope.

Keyworks: Ground vibration; Seismic coefficient; Thuong Tan III quarry; Simulation; Vietnam.

1. Introduction

Blasting is one of the most popular and helpful in fragmenting rocks in open-pit mines. Although the advantages of blasting for rock breakage are undeniable, however, the hazards impacts with blasting are not trivial, such as ground vibration, air overpressure, back-break, fly rock, etc. [1, 2, 3, 4]. Of these undesirable effects, ground vibration is the most dangerous, with many severe impacts, including instability of benches and slopes, disrupting structures, cracks or collapses houses, the vibration of roads and railways, underground water, to name a few. Peak particle velocity (PPV) is well-known as an indicator for measuring ground vibration. It is generated by the wasted energy of explosions and spreads in rocky environments. At high frequencies in a short time, the PPV can significantly affect the structure of the building. Although oscillation is a gradual decrease in the distance, in the case of PPV fluctuations coincide with the natural oscillation of the systems, resonance oscillation will occur and significantly affect cracks, collapses, and subsidence. Consequently, blast-induced PPV evaluation and control are essential to minimize adverse impacts on the environment. Many scholars have studied empirical approaches; however, most models developed for predicting blast-induced PPV were mainly based on the linear relationship between explosive charge per delay and monitoring distance [5, 6, 7].

Therefore, when choosing safe blasting modes, one proceeds from the level of the seismic action of the explosion that does not exceed the maximum permissible value, the existing regulatory data, the actual state of protected objects, their service life, degree of responsibility, etc.

2. Study area and materials

Thuong Tan III quarry is located in Thuong Tan commune, Bac Tan Uyen District, Binh Duong province of Vietnam (Fig. 1). The approved mine reserve is 16.727 million m^3, and the authorized area is 42 ha to

cote -70 m. The deepest mining site reaches -50 m, the soil layer is 4÷5 m thick, and the rock layer is 8÷10 m wide. The stone processing area is located in the south and southwest of the mining area, with the stone crushers in operation. This quarry was selected as a case study because it is close to the Thuong Tan IV quarry with a distance of 180÷200 m [8]. Therefore, blasting operations in the Thuong Tan III quarry were recommended as high risks for the Thuong Tan IV quarry slopes.

In small surveying projects, rotary-wing UAVs such as DJI Phantom 3, 4, or DJI Inspire 2 are often utilized widely [9-16]. Mine terrain for this study is collected in this study is DJI Inspire 2. The camera mounted on the drone is crucially important as it directly contributes to the resulting 3D models' accuracy. The results are shown in Fig. 1.

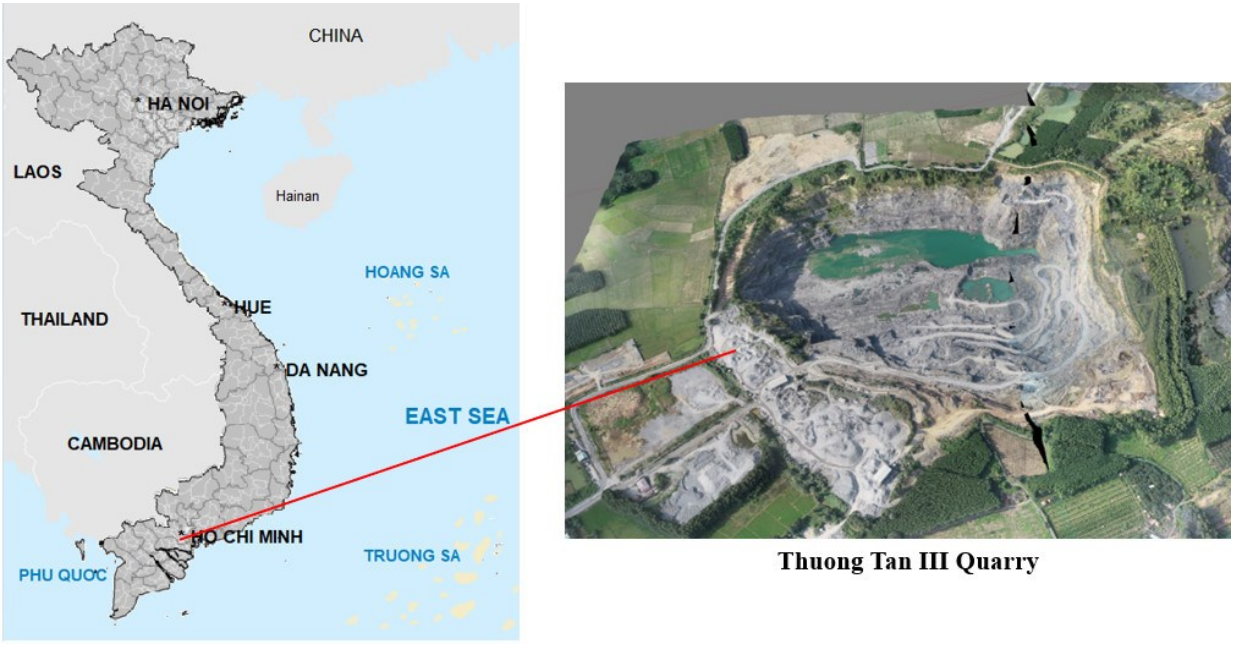

Fig. 1. Location of the Thuong Tan III quarry in Binh Duong province, Vietnam.

In this study, 15 blasting events were performed with a total of 75 explosion-induced ground vibration records at the sensitive environmental objects. The study aimed to determine the attenuation coefficient of blasting vibration (K) to predict the ground vibration caused by the explosion and blast-induced ground vibration at the Thuong Tan III, Thuong Tan IV quarry. We used a multipoint blasting vibration monitoring system (Vibration wireless sensor provides real-time monitoring data- Wireless Mesh Sensor (WMS-02) (Fig. 2):

- Real-Time Wireless Sensors: Sensor products are built to be deployed on mining and construction sites, tunnels, bridges, pathways, and other structures. Sensors also can monitor both vibration and tilt simultaneously. Thanks to this ability, the effects of blasting vibration on structural safety can be understood in real-time [17-19].

- Sensor & Gateway for monitoring & routing: Vibration wireless sensor provides real-time monitoring data. Gateway products quickly route data and alerts to the desired locations (i.e., mobile phones, FTP Server, GIS). USB Management Node is a dongle attached to a PC and establishes a wireless mesh network. It enables bi-directional communication with a maximum of 100 sensors. Sensors have been designed for easy installation and wireless remote management to provide readings and alerts when a user-defined allowable limit is exceeded (Fig. 2).

- Sensors can be positioned over a large area as each sensor can act as a repeater; the sensor network can span kilometers. Multiple sensors are deployed at target locations. Readings are transmitted to the Management Node (Management dongle) connected to the PC. Since our sensors have a built-in router function, all tasks are sent to the detector near the Management Node and, in turn, to the Node (Fig. 3).

Eight blasting events of the mine were conducted, and four seismographs monitored each blasting event. Finally, a total of 75 records of PPV were collected for predicting and simulating the effects of PPV, including the explosive charge per blast (Q), monitoring distance (D), and PPV. It is worth noting that the

Wireless Mesh Sensor (WMS-02) seismograph was used to monitor PPV, and a GPS device was used to measure D. The details of the datasets are summarized in Tab. 1. In this quarry, the borehole diameter of 105 mm, bench height of 8÷10 m, powder factor of 0.35÷0.34 kg/m^3, the burden of 10÷11.5 m, spacing of 2.8÷3.2 m, sub drilling of 105 mm, and stemming of 4.9÷5.2 m; maximum charge per delay Q_{dl}= 20÷40 kg; Total explosives in the blast Q= 1000÷3000 kg; Distance between the blasting and measuring locations R= 100÷500 m. The details of the dataset are presented in Tab. 1.

Fig. 2. Seismograph for monitoring blast-induced ground vibration in the Thuong Tan III quarry.

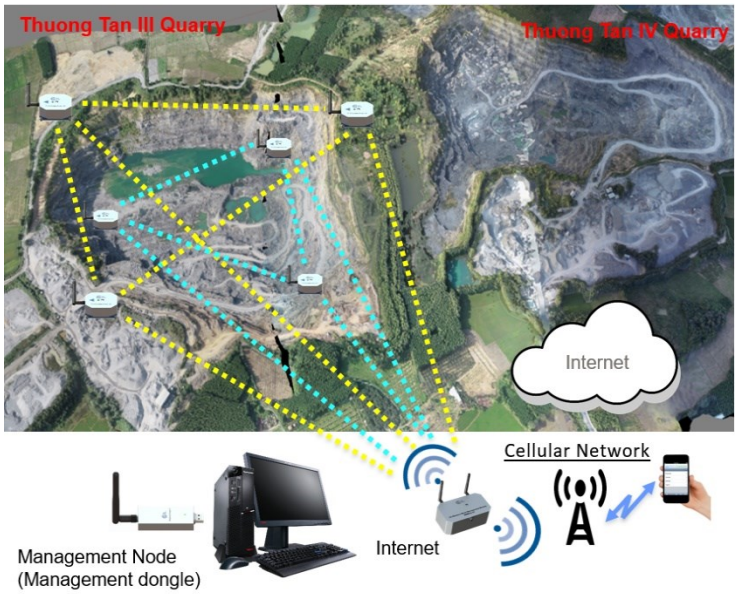

Fig. 3. Scheme for monitoring blast-induced ground vibration in the Thuong Tan III quarry.

Tab. 1. The dataset collected in this study.

Q/Q_{dl}	D	V	Q/Q_{dl}	D	V	Q/Q_{dl}	D	V
2275/ 40	98.25	5.62	2250/ 30	51.3	6.85	1860/ 62	57.4	5.58
	102.93	2.94		75.1	3.55		51.3	6.10
	120.35	1.93		75.3	2.87		32.8	2.80
	56.64	16.85		110.4	1.91		33.9	5.90
	56.14	18.63		24.5	44.84		44.9	3.65
1950/ 27	98.6	1.78	2000/ 38.8	75.1	1.28	1464/ 23	48.3	5.88
	85.7	2.75		62.3	3.64		39.8	12.00
	126.7	1.29		72.0	3.04		44.3	6.13
	93.1	2.08		47.2	5.57		45.3	7.62
	125.3	1.40		31.8	7.08		77.9	5.63
2880/ 36	54.4	6.98	2000/ 31.2	52.4	11.80	2236/ 40	68.4	7.85
	93.4	3.22		50.8	13.05		55.6	14.66
	128.4	4.48		77.5	2.26		33.0	22.68

	78.2	5.37		68.6	2.29		66.2	8.74
	48.7	8.70		63.4	4.87		60.1	9.70
1538/ 48	69.7	6.78	2675/ 29	102.1	3.81	1788/ 40	46.7	3.55
	40.5	13.12		52.0	17.50		43.0	10.20
	65.4	8.30		90.6	14.30		86.5	4.01
	81.3	3.25		74.2	4.12		51.6	3.00
	69.6	3.81		43.0	5.91		33.7	22.20
1760/ 20	44.8	13.05	2625/ 29	73.7	2.43	2700/ 25	84.8	5.04
	64.8	4.87		85.9	24.40		52.5	2.23
	97.3	2.29		71.0	34.20		133.4	4.16
	108.1	1.98		51.8	4.83		161.2	3.10
	78.2	2.26		57.2	3.57		87.0	4.60

3. Methodology

3.1. P-wave and S-wave Velocity Theory in rock

To study the issue more simply, we use methods to analyze the kinematic and dynamic characteristics of elastic waves (deformations) generated in the well by an impulse source. The rock is viewed mainly as a flexible body [20-22]. An elastic body is characterized by the deformations' restoration when the applied forces are removed. In a homogeneous isotropic medium, waves of two types arise and propagate longitudinal wave P and shear wave S (Figs. 4, 5).

- Waves P arise during deformations of the volume of an elastic body. In the P wave, the particles of the medium move in the direction of wave propagation in the applied forces F. The wave is an alternation of compression and extension zones. These zones move at a speed Vp, which is longitudinal wave velocity.
- Waves S waves arise during deformations of the shape (shear) of an elastic body. In the S wave, the particles of the medium move perpendicular to the wave propagation in the direction of the applied forces F. An alternation of stripes with the opposite direction of particle motion is observed. These zones (stripes) move at a speed of Vs. Vs is the speed of the transverse wave.

Fig. 4. Forces and deformations applied (Waves P and waves S).

$$E = (F / S) / (\Delta l / l) \qquad (1)$$

$$\mu = (\Delta d / d) / (\Delta l / l) \qquad (2)$$

Fig. 5. Wave direction and particle movement (Waves P and waves S).

Shear modulus G, Young's modulus E, and Poisson's ratio σ are related. μ- Poisson's ratio can be determined based on measuring the velocities Vp and Vs.

$$G = \frac{E}{2(1+\mu)} \tag{3}$$

$$\mu = \frac{V_P^2 - 2V_S^2}{2(V_P^2 - V_S^2)} \tag{4}$$

- Longitudinal wave P- translational motion of particles of the medium in the direction of propagation of elastic vibrations (waves). Longitudinal waves propagate at a speed Vp determined by the elastic and density properties of the medium [23, 24]:

$$V_p = \sqrt{\frac{E(1-\mu)}{\sigma(1+\mu)(1-2\mu)}} = \sqrt{\frac{\lambda+2\mu}{\sigma}}, \text{ m/s} \tag{5}$$

Transverse wave S - motion of particles of the medium in the direction perpendicular to the propagation of elastic vibrations. Transverse waves propagate at speed V_S determined by the elastic and density properties of the medium [17, 18]:

$$V_s = \sqrt{\frac{E}{\sigma}\frac{1}{2(1+\mu)}} = \sqrt{\frac{\mu}{\sigma}}, \text{ m/s} \tag{6}$$

Where: σ - density of the medium, kg/m^3; λ- Lame constant.

$$\lambda = \frac{\sigma E}{(1+\sigma)(1-2\sigma)} \tag{7}$$

μ - Poisson's ratio (characterizes the resistance of the rock to shape change).

$$\mu = \frac{E}{2(1+\sigma)} \tag{8}$$

E - Young's modulus (Characterizes the resistance of the rock to volume change).
V_p - Longitudinal wave P, m/s
V_s - Transverse wave S, m/s

The constants λ and μ, which determine the rigidity of the medium, grow faster than the density σ during the compaction of rocks. Therefore, an increase in density is usually accompanied by an increase in acoustic velocity. The constants λ and μ are always positive. Consequently, the speeds of the longitudinal waves are always more significant than the velocities of the transverse ones.

Seismic coefficient (K) changes depending on the change in the blasting conditions. K is determined based on specific measurements of the velocity with known Q and R. When calculating the seismic effect of short-delay explosions, if there is no data on the maximum weight of the charge in the group, the values of the seismicity coefficients can be determined through the function of reducing the seismic effect of explosions. Then the value of the seismicity coefficient is found by the formula:

$$K = 1000.\sqrt[3]{\frac{V_p}{\sigma}(1-\frac{4}{3}\frac{V_s}{V_p})^2} \tag{9}$$

3.2. Empirical model for estimating blast-induced ground vibration

To estimate blast-induced ground vibration by empirical methods, the well-known formula of M.A. Sadovsky [25-27] was used in this study and is described in Eq. 10.

$$V = K\left(\frac{R}{\sqrt[3]{Q_{dl}}}\right)^{-\alpha}, \text{ mm/s} \tag{10}$$

where: V- peak particle velocity, mm/s; Q_{dl}- maximum charge per delay, kg; R- the distance between the blasting and measuring locations, m; K- seismic coefficient, α- specific geological constant; D-Scaled

distance, $D = R / \sqrt[3]{Q_{dl}}$.

3.3. Simulation of blast-induced ground vibration effects

To evaluate the effects of blast-induced ground vibration on the surrounding environment, the slope stability in the Thuong Tan III quarry [28-30] was simulated through the numerical analysis model using the Phase 2 software. For this aim, the equivalent blasting pressure (P_f) is calculated based on Eq. 11:

$$P_f = 0.0037 \rho v^2 \qquad (11)$$

where ρ - Density of explosion; v - Velocity of the explosion, fps.
It is worth mentioning that P_f is calculated and used in the Phase 2 software under the effects of Q_{dl}, which is one of the simulation model inputs.

4. Results and discussion

4.1. Determination of the seismic coefficient (K) based on rock properties

Through exploration results up to cote -100m, it was shown that the mineral body of the stone-built in the mine is siltstone, claystone, claystone contains little lime accounted for 68 %. The thickness of the layer of siltstone containing lime is from a few cm to >10m. The siltstone containing little lime are rocks with technological properties that meet the standards for use as building materials for concrete aggregates requiring high bearing properties (type I stone). The remaining rocks include siltstone clay containing little lime, having lower compressive strength (grade II rock), accounted for 32 % that meets the standard for being used as common building materials for construction (Fig. 6).

Fig. 6. Rock properties of the Thuong Tan III quarry.

The thickness of the siltstone layer, siltstone containing lime, is from a few cm to >10 m. The siltstone, siltstone containing little lime, siltstone, and siltstone containing little lime are rocks with technological properties that meet the standards for use as building materials for concrete aggregates requiring high bearing properties (type I stone). The remaining rocks include siltstone clay, siltstone clay containing little lime, claystone, claystone containing less lime, having lower compressive strength (grade II rock) accounted for 32% that meets the standard for being used as common building materials for construction, civil construction, and rural transport.

- Siltstone: V_p = 3540 m/s; V_s = 1880 m/s; σ = 2720 kg/m^3
- Clay-Siltstone: V_p = 3260 m/s; V_s = 1722 m/s; σ = 2680 kg/m^3
- Claystone: V_p = 3015 m/s; V_s = 1690 m/s; σ = 2540 kg/m^3

In the Thuong Tan III quarry, the majority rocks are siltstone, clay-siltstone, and claystone. Eq. 9 was applied to calculate the K values, as shown in Tab. 2.

Tab. 2. Seismic coefficient of the Thuong Tan III quarry based on the rock properties.

Value	Type of stone		
	Siltstone	**Clay-Siltstone**	**Claystone**
σ, kg/m^3	2720	2680	2540
V_p, m/s	3240	2855	2515
V_s, m/s	1880	1722	1690
K	*713*	*656*	*539*

From Tab. 1, it can be seen that K when blasting with siltstone is higher (1.02÷1.11) times than that of clay-siltstone and claystone.

4.2. Determination of the seismic coefficient (K) based on the empirical model

To determine the K based on the empirical model, the empirical equation (10) can be expanded as follows:

$$K = \frac{VR^{\alpha}}{Q_{dl}^{\frac{\alpha}{3}}} \tag{12}$$

Based on the experimental datasets and empirical equation (10), blast-induced ground vibration can be calculated according to Eq. 13, and the relationship between V and D (Fig. 7).

$$V = 626.13\left(\frac{R}{\sqrt[3]{Q}}\right)^{-1.14}, \text{ mm/s} \tag{13}$$

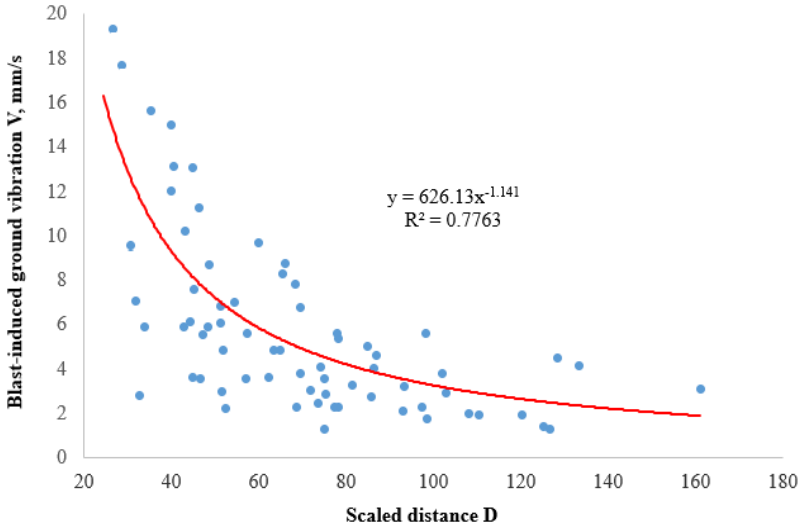

Fig. 7. Relationship between V and Scaled distance D.

Based on Eq. 13, it is easy to see that K= 626.13 and the specific geological constant α= -1.14. Next, Eq. 12 was applied to calculate K values, as listed in Tab. 3.

Tab. 3. The dataset collected for this study.

Q/Q_{dl}	D	V	K	Q/Q_{dl}	D	V	K	Q/Q_{dl}	D	V	K
2275/40	98.25	5.62	*1054*	2250/30	51.3	6.85	*612*	1860/62	57.4	5.58	*566*
	102.93	2.94	*582*		75.1	3.55	*490*		51.3	6.10	*545*
	120.35	1.93	*456*		75.3	2.87	*398*		32.8	2.80	*150*
	56.64	16.85	*1686*		110.4	1.91	*410*		33.9	5.90	*329*
	56.14	18.63	*1846*		24.5	44.84	*1724*		44.9	3.65	*280*
1950/27	98.6	1.78	*335*	2000/38.8	75.1	1.28	*177*	1464/23	48.3	5.88	*490*
	85.7	2.75	*442*		62.3	3.64	*406*		39.8	12.00	*804*
	126.7	1.29	*322*		72.0	3.04	*400*		44.3	6.13	*463*
	93.1	2.08	*367*		47.2	5.57	*453*		45.3	7.62	*591*
	125.3	1.40	*347*		31.8	7.08	*367*		77.9	5.63	*811*
2880/36	54.4	6.98	*667*	2000/31.2	52.4	11.80	*1081*	2236/40	68.4	7.85	*974*
	93.4	3.22	*570*		50.8	13.05	*1153*		55.6	14.66	*1436*
	128.4	4.48	*1142*		77.5	2.26	*323*		33.0	22.68	*1227*
	78.2	5.37	*777*		68.6	2.29	*285*		66.2	8.74	*1045*
	48.7	8.70	*733*		63.4	4.87	*554*		60.1	9.70	*1039*

1538/48	69.7	6.78	*859*	2675/29	102.1	3.81	*747*	1788/40	46.7	3.55	*285*
	40.5	13.12	*896*		52.0	17.50	*1590*		43.0	10.20	*746*
	65.4	8.30	*980*		90.6	14.30	*2445*		86.5	4.01	*651*
	81.3	3.25	*491*		74.2	4.12	*560*		51.6	3.00	*270*
	69.6	3.81	*483*		43.0	5.91	*432*		33.7	22.20	*1229*
1760/20	44.8	13.05	*1000*	2625/29	73.7	2.43	*329*	2700/25	84.8	5.04	*800*
	64.8	4.87	*569*		85.9	24.40	*3927*		52.5	2.23	*204*
	97.3	2.29	*425*		71.0	34.20	*4426*		133.4	4.16	*1106*
	108.1	1.98	*414*		51.8	4.83	*437*		161.2	3.10	*1023*
	78.2	2.26	*327*		57.2	3.57	*361*		87.0	4.60	*751*

4.3. Simulation of slope stability based on the K and blast-induced ground vibration

Slope stability is considered one of the most adverse effects of blast-induced ground vibration on the surrounding environment. A slope failure in a mine working area can give rise to significant economic losses and safety impacts. The fundamental failure modes are varied and complex. Such mechanisms are governed by engineering geology conditions of rock mass which are almost always unique to a particular site. Using a numerical analysis model of the finite element method under the Phase 2 environment, we simulated the effects of blast-induced ground vibration on slope stability.

Accordingly, Eq. 11 was applied based on the maximum explosive charged per blast for this aim. Based on Eq. 11, ground vibration, and K, different scenes can be applied to simulate the equivalent blasting pressure. As an example, Q = 1000 kg, P_f = 3.325 MPa. The results are simulated in Fig. 8.

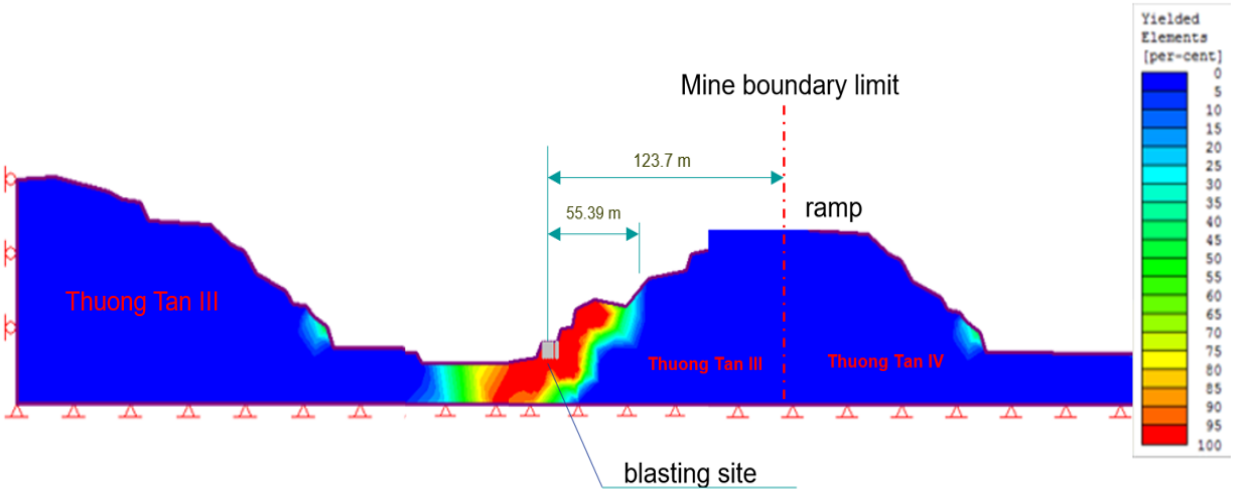

Fig. 8. Simulation of slope stability with Q= 1000 Kg.

As shown in Fig. 8, it is clear that the impact zone of blast-induced ground vibration with the Q_{max} = 1000 kg is in the range of 0 to 55.39 m. Therefore, the safety distance for slopes in the Thuong Tan III quarry with Q_{max} = 1000 kg is R > 55.39 m (Tab. 4).

Tab. 4. The blasting distance ensures the safety and stability of the slope for Thuong Tan III.

№	**Parameter**	**Safety distance**	
1	Distance from blasting site to slope stability	R≥ 55.39 m	R< 55.39 m
2	Maximum charge per delay	$Q_{dl} \leq$ 40 kg	$Q_{dl} \leq$ 30 kg
3	Maximum explosive charged per blast	1000 kg< Q ≤ 3000 kg	Q≤ 1000 kg (Presplit Blasting)

5. Conclusions

Blasting is a crucial stage in the mining process; nevertheless, its side effects, especially blast-induced ground vibration, need to accurately predict and controlled to reduce the damages induced by blasting operations. Based on the results of this study, we draw some conclusions:

- Attenuation coefficient of blasting vibration (K) changes depending on the change in the blasting conditions. K is determined based on specific measurements of the velocity with known Q and R. We can determine the vibration attenuation coefficient due to blasting (K= 539÷713) when blasting for each different type of rock (Siltstone, Clay-siltstone, Claystone). As a result, we can predict a safe zone of earthquake vibration due to the above explosion affecting the stamina slope stability.

- In this study, we used a multipoint blasting vibration monitoring system (Vibration wireless sensor provides real-time monitoring data). It is possible to determine the attenuation coefficient of blasting vibration K to predict the intensity and safety zone of blast-induced ground vibration in a quarry from test blasting results.

- Using a numerical analysis model of the finite element method (Phase 2), we simulate the effect of the blasting pressure values on the slope stability of the Thuong Tan III quarry as well as the safety zone of blast-induced ground vibration in the quarry. Based on the obtained results, sensitive environmental objects can be protected and safe during the mining process.

Several techniques are used to improve wall stability in open-pit mines. Pre-split blasting is the most pragmatic and practical approach for tackling this issue in open-pit mines.

6. Acknowledgements

The author would like to acknowledge and appreciate the opinions and judgments of researchers, scientists, and professors who came from Dong-A University, Korea, and Hanoi University of Mining and Geology. This paper would not have been possible without experiences and support from professors, experts, researchers, and engineers. In addition, the author thanks peer-reviewers for their valuable comments, which helped us improve the manuscript's quality.

The paper was presented during the 6th VIET - POL International Conference on Scientific-Research Cooperation between Vietnam and Poland, 10-14.11.2021, HUMG, Hanoi, Vietnam.

7. References

1. Bui, X.-N., Choi, Y., Atrushkevich, V., Nguyen, H., Tran, Q.-H., Long, N. Q., et al., 2020. Prediction of Blast-Induced Ground Vibration Intensity in Open-Pit Mines Using Unmanned Aerial Vehicle and a Novel Intelligence System. Natural Resources Research, 29(2): 771-790, doi:10.1007/s11053-019-09573-7.
2. Nguyen, H., Bui, X.-N., & Moayedi, H., 2019a. A comparison of advanced computational models and experimental techniques in predicting blast-induced ground vibration in open-pit coal mine. [journal article]. Acta Geophysica, 67(4): 1025-1037, doi:10.1007/s11600-019-00304-3.
3. Nguyen, H., Bui., X.-N., Tran, Q.-H., Le, T.-Q., & Do, N.-H., 2019b. Evaluating and predicting blast-induced ground vibration in open-cast mine using ANN: A case study in Vietnam. SN Applied Sciences, 1(1): 125.
4. Ding, Z., Nguyen, H., Bui, X.-N., Zhou, J., & Moayedi, H., 2020. Computational Intelligence Model for Estimating Intensity of Blast-Induced Ground Vibration in a Mine Based on Imperialist Competitive and Extreme Gradient Boosting Algorithms. Natural Resources Research, 29(2): 751-769, doi:10.1007/s11053-019-09548-8.
5. Armaghani, D. J., Momeni, E., Abad, S. V. A. N. K., & Khandelwal, M., 2015. Feasibility of ANFIS model for prediction of ground vibrations resulting from quarry blasting. Environmental Earth Sciences, 74(4): 2845-2860.
6. Khandelwal, M., & Singh, T., 2006. Prediction of blast induced ground vibrations and frequency in opencast mine: a neural network approach. Journal of sound and vibration, 289(4): 711-725.
7. Monjezi, M., Hasanipanah, M., & Khandelwal, M., 2013. Evaluation and prediction of blast-induced ground vibration at Shur River Dam, Iran, by artificial neural network. Neural Computing and Applications, 22(7-8): 1637-1643.

8. Evaluation of the impact during and after mining on the cote -100m of Thuong Tan III and Thuong Tan IV quarries, Thuong Tan commune, Bac Tan Uyen district, Binh Duong province, Code 3209/QD-UBND Binh Duong, Chairman, Acceptance 24/01/2019.
9. Bui Xuan Nam., Lee Changwoo., Nguyen Quoc Long., Adeel Ahmad., Cao Xuan Cuong., Nguyen Viet Nghia., Le Van Canh., Nguyen Hoang., Le Qui Thao., Duong Thuy Huong., Nguyen Van Duc., 2019. Use of Unmanned Aerial Vehicles for 3D topographic Mapping and Monitoring the Air Quality of Open-pit Mines, Inzynieria Mineralna, 2: 222-238.
10. Nguyen Quoc Long., Ropesh Goyal., Bui Khac Luyen., Le Van Canh., Cao Xuan Cuong., Pham Van Chung., Bui Ngoc Quy., Xuan-Nam Bui., 2020. Influence of Flight Height on The Accuracy of UAV Derived Digital Elevation Model of Complex Terrain, Inzynieria Mineralna, 1: 179-187.
11. Le Van Canh., Cao Xuan Cuong., Le Hong Viet., Dinh Tien., 2020. Volume computation of quarries in Vietnam based on Unmanned Aerial Vehicle (UAV) data (in Vietnamese). Journal of Mining and Earth Sciences. 61, 1: 21-30. DOI:https://doi.org/10.46326/JMES.2020.61(1): 03.
12. Nguyen Quoc Long., Vo Ngoc Dung., Vo Chi My., 2020. Advanced Mining Geomatic Technologies Serving Open-Pit Mining Operation in Vietnam (in Vietnamese). Journal of Mining and Earth Sciences. 61(5): 125-133. DOI:https://doi.org/10.46326/JMES.KTLT2020.11.
13. Nguyen Viet Nghia., 2020. Building DEM for deep open-pit coal mines using DJI Inspire 2 (in Vietnamese). Journal of Mining and Earth Sciences. 61(1): 1-10. DOI:https://doi.org/10.46326/JMES.2020.61(1).01.
14. L. Q. Nguyen, 2021. Accuracy assessment of open - pit mine's digital surface models generated using photos captured by Unmanned Aerial Vehicles in the post - processing kinematic mode (in Vietnamese). Journal of Mining and Earth Sciences, Vol. 62, no. 4, Aug. 2021, p 38-47, doi:10.46326/JMES.2021.62(4).05.
15. Nguyen, Q. L., Le, T. T. H., Tong, S. S., Kim, T. T. H., (2020). UAV Photogrammetry-Based For Open Pit Coal Mine Large Scale Mapping, Case Studies In Cam Pha City, Vietnam. Sustainable Development of Mountain Territories, 12(4), 501-509. DOI: 10.21177/1998-4502-2020-12-4-501-509.
16. Nguyen Q. L., Ropesh G., Bui, K. L, Cao X. C., Le V. C., Nguyen Q. M., Xuan-Nam B., (2021). Optimal Choice of the Number of Ground Control Points for Developing Precise DSM using Light-Weight UAV in Small and Medium-Sized Open-Pit Mine. Archives of Mining Sciences, 66 (3), p 369-384, doi: 10.24425/ams.2021.138594.
17. Tran Quang Hieu., Hoang Nguyen., Xuan-Nam Bui., Carsten Drebenstedt., Belin Vladimir Arnoldovich., Victor Atrushkevich., 2021. Evaluating the Effect of Meteorological Conditions on Blast-Induced Air Over-Pressure in Open Pit Coal Mines, Xuan-Nam Bui et al. (Eds.): Proceedings of the International Conference on Innovations for Sustainable and Responsible Mining. 1, Springer (indexed by Scopus), https://doi.org/10.1007/978-3-030-60839-2_9.
18. Nguyen Hoang., Bui Xuan Nam., Tran Quang Hieu., Le Thi Huong Giang., 2020. A novel soft computing model for predicting blast - induced ground vibration in open - pit mines using gene expression programming (in Vietnamese). Journal of Mining and Earth Sciences. 61(5): 107-116. DOI:https://doi.org/10.46326/JMES.KTLT2020.09.
19. Tran Quang Hieu., Bui Xuan Nam., Nguyen Hoang., Nguyen Anh Tuan., Nguyen Quoc Long., 2020. Applicable posssibility of advanced technologies and equipment in surface mines of Vietnam. Journal of Mining and Earth Sciences. 61(5): 16-32. DOI:https://doi.org/10.46326/JMES.KTLT2020.02.
20. Carcione, J.M., Tinivella, U., 2000. Bottom simulating reflectors: seismic velocities and AVO effects. 65: 54-67.
21. С.В. Густов., Л.В., 2012. Суровицкий. Влияние диаметра заряда на коэффициент, характеризующий кдельный сейсмический эффект в управнении садовоооского,– 61 с.
22. Лобова Г.А., 2012. Полевая геофизика и геофизические исследования скважин: методические указания по выполнению домашнего задания по дисциплинам «Полевая геофизика» и «Геофизические исследования скважин» (заочная форма обучения). – Томский политехнический университет, 16с.

23. J.P.Castagna., M.L. Batzle., and R.L.Eastwood., 1985. Relationship between compressional-wave and shearwave velocities in clastic silicate rocks, Geophysics, 50: 571-581.
24. Per Avseth., et al., 2008. "Quantitative Seismic Interpretation", Cambridge University Press, 2005P.F. Anderson and L.R. Lines, "A comparison of inversion techniques for estimating Vp/Vs from 3D seismic data", CREWES Research Report. 20.
25. Dam Trong Thang., Bui Xuan Nam., Tran Quang Hieu., 2014, Blasting in mining and structures. Publishing house of natural and technology science. Ha Noi. 454.
26. QCVN 01:2019/BCT., National technical regulation on safety in the storage, transportation, use and disposal of industrial explosive materials.
27. Садовский М.А., 2004. Оценка сейсмически опасных зон при взрывах // В кн. М.А.Садовский. Избранные труды: Геофизика и физика взрыва. - М.: Наука. С. 93-102.
28. Le Dinh Tan., 2000. The dynamic calculation of underground structures under impacting of blasting wave. Doctor thesis. Military Technical Academy. Ha Noi.
29. Martin Stolárik,. Modeling of vibration effect within small distances, Acta Geodyn. Geomater. 2008. 5(2): 137-146.
30. Tran Tuan Minh., Bui Xuan Nam., Tran Quang Hieu., Nguyen Quang Huy., 2018. Research on the effects of the blasting pressure values on the stability of concrete lining in the existing tunnel during expansion auxiliary tunnel in Hai Van pass project of Viet Nam, Журнал «Устойчивое развитие горных территорий», 3(37): 411-419.

http://doi.org/10.29227/IM-2021-02-54 Received: 16 Jun 2021, Accepted: 18 Aug 2021, Published: 10 Nov 2021